Electromagnetic Pulses Produced by Bouncing-Wave-Type Lightning Discharges

Amitabh Nag, *Member, IEEE*, and Vladimir A. Rakov, *Fellow, IEEE*

(Invited Paper)

***Abstract*—Based on experimental evidence of multiple reflections and modeling, we infer that the so-called compact intracloud lightning discharge (CID) is essentially a bouncing-wave phenomenon. Some tens of reflections may occur at both radiating-channel ends. The reflections have little influence on the overall CID electric field signature (narrow bipolar pulse (NBP) waveform), but are responsible for its fine structure, "noisiness" of dE/dt waveforms, and accompanying HF–VHF radiation bursts.**

***Index Terms*—Electric field derivative, HF–VHF radiation, lightning discharge, lightning electromagnetic (EM) pulse, traveling wave, wave reflections.**

I. Introduction

THERE is a distinct class of lightning discharges that are referred to as compact intracloud discharges (CIDs). These discharges were first reported by Le Vine [7], and later characterized by Willett *et al.* [15] and Smith *et al.* [10], [11], among others. Salient properties of these discharges can be summarized as follows (see [6] and [9]).

1) They are the most intense natural producers of HF–VHF (3–300 MHz) radiation on Earth.
2) They produce single bipolar electric field pulses of either initial half-cycle polarity (so-called narrow bipolar pulses or NBPs) having typical full widths of 10–30 μs and amplitudes of the order of 10 V/m at 100 km.
3) They produce very "noisy" dE/dt signatures, while the corresponding electric field signatures are relatively smooth.
4) They tend to occur in isolation and at high altitudes (mostly above 10 km).
5) They do not occur in locations (e.g., Sweden) where cloud tops are relatively low.
6) They appear to be associated with strong convection, possibly with convective surges overshooting the tropopause and penetrating deep into the stratosphere; however, even the strongest convection does not always produce CIDs.
7) They tend to produce less light than other types of lightning discharges.

The mechanism of CIDs remains elusive. There were attempts to model CIDs as runaway electron avalanches initiated by energetic electrons (e.g., cosmic ray secondaries) in thundercloud electric fields (e.g., [1], [3], [4], and [12]). However, model-predicted wideband (extremely low frequency (ELF)–low frequency (LF): 3–300 kHz) electric field waveforms are inconsistent with measurements. A reasonable agreement with observations in terms of the overall NBP (VLF–LF) waveform was achieved by using transmission-line-type models and assuming matched conditions (total absorption) at the far channel end [7], [14]. However, these simple models do not address the issues of NBP fine structure, "noisiness" of dE/dt waveforms, and accompanying HF–VHF radiation bursts. It appears that the CID is the most mysterious, but also potentially hazardous, type of lightning. According to Willett *et al.* [15], electromagnetic (EM) pulses produced by CIDs could pose a serious threat to airspace vehicles, whose fundamental structural resonances usually lie at HF (3–30 MHz).

In this paper, we propose the bouncing-wave mechanism for generation of EM pulses by CIDs. Vertical electric fields at ground level predicted by this mechanism at both close and far distances from the source are consistent with the available experimental data [2], [8].

II. Evidence of Reflections in EM Field Signatures

Hamlin *et al.* [5] reported that 12% of their CIDs showed evidence of current reflections, which appeared as a secondary pulse after the initial peak in their distant electric field waveforms. They interpreted the secondary pulse as a signature of reflection of source current pulse off the far end of the CID channel, and used this feature to estimate CID channel length. We searched for secondary pulses in our data and found evidence of not just one, but multiple (up to seven) reflections off both the ends of the CID channel. Our pulse detection efficiency was considerably higher than Hamlin *et al.*'s, because, in addition to electric fields (E), we used our dE/dt records. We found that Hamlin *et al.*'s secondary peak is actually a higher order one, and therefore, it would result in an overestimate if used for calculating the radiator length.

In Fig. 1, we present (a) electric field, (b) dE/dt, and (c) VHF radiation burst produced by one of the CIDs in our dataset. For this event, the initial polarity of NBP [see Fig. 1(a)] is the same as that of negative return strokes, and is consistent with motion of negative charge downward (or positive charge upward). The overall pulse duration is about 16 μs, which is within the range of typical values, 10–30 μs, for NBPs. A superposition of the E, dE/dt, and VHF signatures is shown in Fig. 1(d).

Manuscript received May 21, 2009. First published July 31, 2009; current version published August 21, 2009. This work was supported in part by the National Science Foundation and in part by the Defense Advanced Research Projects Agency.

The authors are with the Department of Electrical and Computer Engineering, University of Florida, Gainesville, FL 32611 USA.

Color versions of one or more of the figures in this paper are available online at http://ieeexplore.ieee.org.

Digital Object Identifier 10.1109/TEMC.2009.2025495

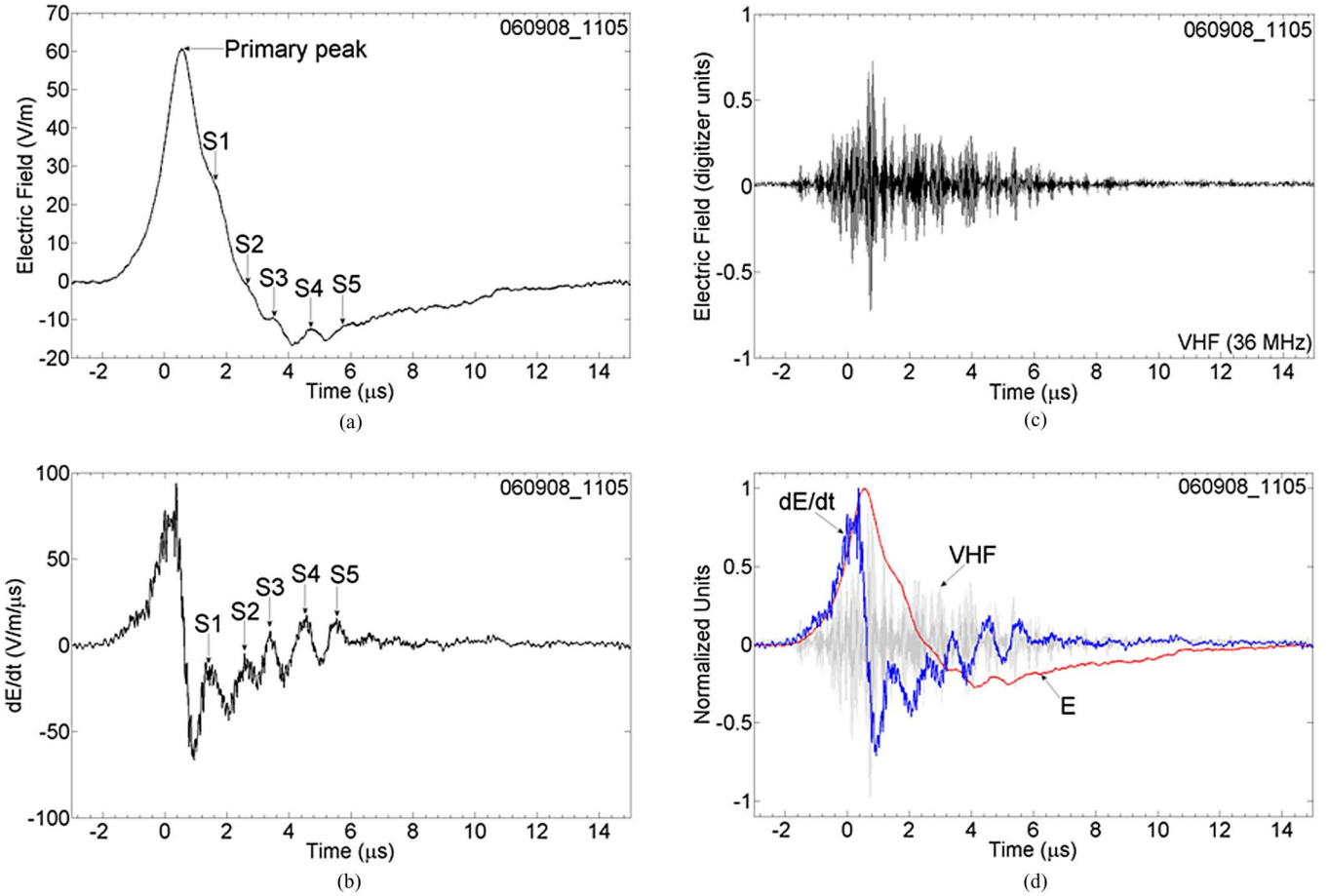

Fig. 1. (a) Vertical electric field. (b) dE/dt. (c) VHF radiation signatures of a CID recorded in Gainesville, FL. It occurred at an unknown distance and transferred negative charge downward. The three signatures are overlaid in (d) for direct comparison, with the VHF being lighter, so that it does not obscure the other two signatures. S1–S5 are five secondary peaks appearing as pronounced oscillations in (b) and mostly as shoulders in (a).

Note that the VHF burst starts about the same time as the NBP (VLF–LF signature) and continues throughout most of its duration. The electric field measuring system had a useful frequency bandwidth of 16 Hz to 10 MHz. The upper frequency response of the dE/dt system was 17 MHz. The VHF system had a −3-dB bandwidth of 34–38 MHz.

At least one secondary peak (labeled S4) having the same polarity as the primary peak and multiple shoulders (labeled S1–S3 and S5) are seen in Fig. 1(a). In the dE/dt signature [see Fig. 1(b)], secondary peaks appear as pronounced oscillations after the initial opposite polarity (negative) overshoot. There are five pronounced cycles in Fig. 1(b), whose positive half-cycles are labeled S1–S5. The first three of them correspond to shoulders S1–S3, and the following one to the secondary peak S4 in Fig. 1(a). Note that the peaks in the E-field waveform correspond to local "zeroes" in the dE/dt waveform [see Fig. 1(d)]. We found multiple secondary peaks (oscillations) in 32 (15%) of our dE/dt records. Factors that can make reflections undetectable in the remaining 85% include a relatively small magnitude of the incident wave, relatively long radiating channel length and/or stronger attenuation along the channel, and a relatively small (in absolute value) current reflection coefficient. We found, via modeling, that the channel length is unlikely to exceed several hundred meters. The current reflection coefficient should be in the range from 0 to −0.5. When reflections were detectable, the time interval between consecutive peaks of the same polarity in dE/dt signatures ranged from 0.64 to 2.3 μs with a mean of 1.2 μs. We found, via modeling, that the multiple peaks (oscillations) are due to reflections at either end of CID channel, with the time interval between consecutive peaks (oscillation period) being equal to the round-trip time along the channel. Interestingly, the period of oscillations remains more or less constant [see Fig. 1(b)], implying that the radiator length remains fixed during the bouncing-wave process.

III. Bouncing-Wave Mechanism

Based on the evidence of multiple reflections, we postulate that the CID is essentially a bouncing-wave phenomenon. It can be viewed as beginning with injection of a current pulse at one end of a relatively short conducting channel, which is reflected multiple times successively at either end of the channel until it is attenuated and absorbed, depending upon the conditions along the channel and boundary conditions at channel ends, respectively. The concept is illustrated by four schematic snapshots in Fig. 2 for the case of vertical channel of length equal to 100 m

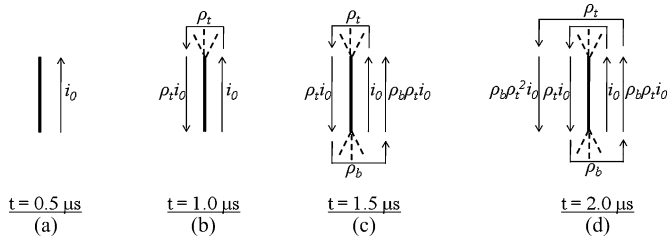

Fig. 2. Schematic representation of the bouncing-wave mechanism of CID for discharge channel length $\Delta h = 100$ m and propagation speed $v = 2 \times 10^8$ m/s. Current-wave duration is much longer than the channel traversal time. Straight arrows represent current waves on CID channel and bracket-shaped arrows represent the process of wave reflection at the ends. If $\rho_b = \rho_t = 1$ (short-circuit conditions), it is the same wave bouncing between the ends. If $\rho_b = \rho_t = -1$ (open-circuit conditions), the wave changes polarity each time it hits the end. If $\rho_b = \rho_t = -0.5$, the current wave changes polarity and is reduced in magnitude by a factor of 2 at each end. If $\rho_t = 0$, the wave is fully absorbed at the top end. For $|\rho_t| < 1$ and $|\rho_b| < 1$, partial absorption takes place at the top and bottom, respectively. It is expected that reflected current waves will reduce current at each end, while corresponding voltage will be enhanced there. As a result, corona-like electrical breakdown (shown by broken lines) may occur at the channel ends. Breakdown associated with the incident wave i_0 is not shown here.

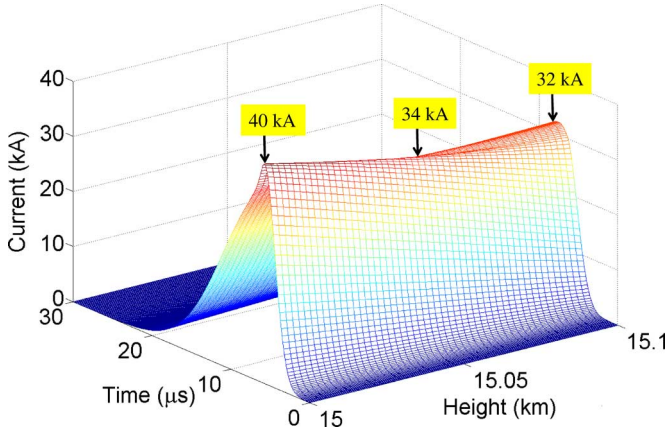

Fig. 3. Total current (including reflections) as a function of time and height for a CID characterized by $h_1 = 15$ km, $\Delta h = 100$ m, $v = 2 \times 10^8$ m/s, $\rho_b = \rho_t = -0.5$, $I_p = 50$ kA, and RT $= 6$ μs. See text for details.

and propagation speed equal to 2×10^8 m/s, which corresponds to a round-trip time of 1 μs. The pulse duration is much larger than the time required for the pulse to traverse the channel (the pulse rise time is expected to be several microseconds, while the traversal time for this case is 0.5 μs).

The incident current pulse i_0 travels upward, so that the front of the pulse will reach the top of the channel at $t = 0.5$ μs. The instant just before the pulse arrival at the top is shown in snapshot Fig. 2(a). At the top of the channel, the pulse will "see" an impedance discontinuity, and hence, will be, in general, partly reflected. The front of the pulse (scaled according to the reflection coefficient at the top of the channel) will move downward. The downward motion will continue till $t = 1$ μs [see Fig. 2(b)], at which time the pulse will hit the bottom of the channel, where it will be reflected again and will begin to travel upward [see Fig. 2(c)]. The second reflection at the top and resultant downward motion are depicted in snapshot Fig. 2(d). Note that while the initial parts of the pulse have already experienced multiple reflections, later portions are still making their first trip upward or did not even enter the bottom of the channel. After $t = 0.5$ μs, in addition to the upward moving incident wave (i_0), different portions of the pulse (scaled according to corresponding reflection coefficients) will be traveling either downward or upward after being reflected from the top or the bottom of the channel, respectively.

Reflections of different portions of current pulse are likely to result in corona-like electrical breakdown at channel extremities, because a reduction of current is accompanied by an increase of line charge density and associated voltage (voltage doubles at an open-circuit end and increases by a factor of 1.5 if the current reflection coefficient is equal to -0.5). We infer that this breakdown at both channel ends will produce a burst of HF–VHF radiation, concurrent with the NBP, which is a characteristic feature of CIDs [see Fig. 1(c)]. Multiple reflections and resultant breakdown at radiator ends also help to explain the unusual "noisiness" of dE/dt waveforms, a CID feature first noticed by Willett *et al.* [15].

IV. Distribution of Current Along the Channel

As an example, let us consider a current pulse with a peak (I_p) of 50 kA, total duration of 30 μs, and rise time (RT) of 6 μs, injected at the bottom of a 100-m-long vertical conducting channel. We assume that the bottom of the channel is at an altitude (h_1) of 15 km, and that negative charge is transferred upward (the most common scenario). The pulse travels upward at an assumed speed of 2×10^8 m/s (we found, via modeling, that this parameter should be between about 10^8 m/s and the speed of light). Let the current reflection coefficients at the top and the bottom of the channel be constant and equal to -0.5. We do not consider losses in the channel, assuming that the reflection coefficients effectively account for both the channel losses and absorption at channel ends. Breakdown at channel ends should alter the reflection coefficients (making them nonlinear), but we neglect this effect here.

A 3-D plot of the resultant total current (including all the reflections), as a function of time and height above ground, is shown in Fig. 3. Note that current peaks at the bottom, midpoint, and top of the channel are 40, 34, and 32 kA, respectively, versus 50-kA peak of the incident wave.

V. Electric Fields at 2 and 200 km

Vertical electric fields produced at ground at horizontal distances of 2 and 200 km from an elevated vertical source, whose spatiotemporal current distribution is shown in Fig. 3, are presented in Fig. 4. Additionally, shown in Fig. 4 are the three field components (electrostatic, induction, and radiation) at 2 km and dE/dt waveform at 200 km. The fields were calculated using a general equation for a differential channel segment (e.g., [13]), which was integrated over the radiating channel length, taking into account all the relevant reflections from the ends. At 2 km [see Fig. 4(a)], the electric field is dominated by its induction component at earlier times (up to 20 μs or so), and becomes essentially electrostatic after 25 μs. Contribution from

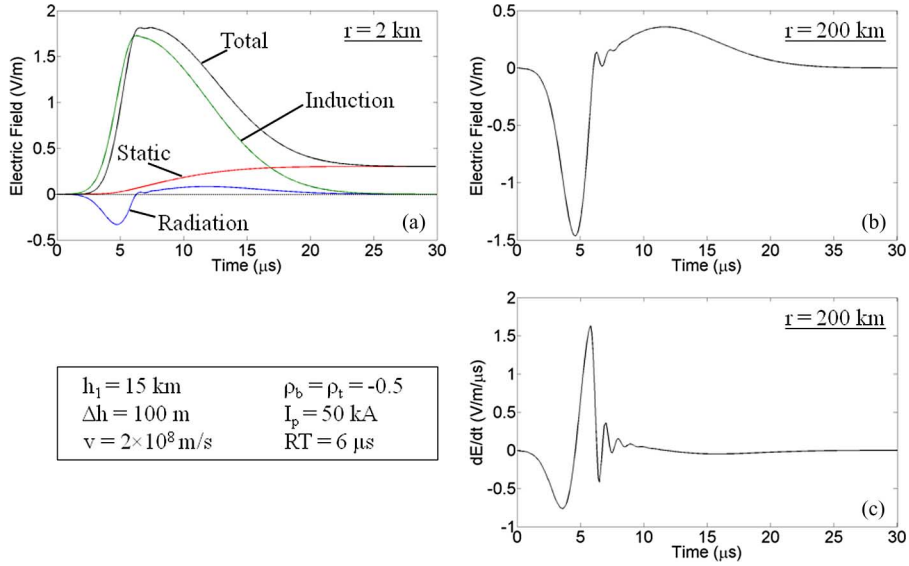

Fig. 4. (a) Total vertical electric field at ground and its three components at a horizontal distance of 2 km. (b) and (c) Total vertical electric field (essentially the same as its radiation component) and its time derivative, respectively, at 200 km for the CID whose parameters are listed in the box and whose spatiotemporal current distribution is shown in Fig. 3. The event transferred negative charge upward.

the radiation component is mostly negligible; it is the largest around 5 μs and almost zero after the total field peak. Note that the initial polarity of the radiation component is opposite to that of the electrostatic and induction components, as expected at close distance from an elevated vertical source. At 200 km [see Fig. 4(b)], the total electric field is essentially the same as its radiation component and exhibits two secondary peaks due to reflections at channel ends. More evidence of reflections is seen in Fig. 4(c). Note that, in 10 μs, a total of 20 reflections have occurred, ten at the top and ten at the bottom, but only a few of them are evident in Figs. 4(b) and (c). Thus, the reflections have little influence on the overall CID electric field signature (NBP waveform), although they are responsible for its fine structure, as well as, by inference, for "noisiness" of dE/dt waveforms and for accompanying HF–VHF radiation bursts. The latter two features should become more pronounced as the current reflection coefficients approach -1 (open-circuit conditions at the ends). The computed electric field waveforms at 2 and 200 km [see Figs. 4(a) and (b)] are qualitatively consistent with CID electric field waveforms measured at similar distances by Eack [2] and others.

VI. Summary

There is a distinct class of lightning discharges that are referred to as CIDs. These discharges are the most intense natural producers of HF–VHF radiation on Earth. They also produce VLF–LF electric field pulses (so-called NBPs) having typical full widths of 10–30 μs and amplitudes of the order of 10 V/m, when normalized to100 km. Based on the experimental evidence of multiple reflections and modeling, we infer that the CID is essentially a bouncing-wave phenomenon. Some tens of reflections may occur at both radiating-channel ends. The reflections have little influence on the overall CID electric field signature (NBP waveform), but are responsible for its fine structure, "noisiness" of dE/dt waveforms, and accompanying HF–VHF radiation bursts.

Acknowledgment

The authors would like to thank D. Tsalikis for his help in developing instrumentation and acquiring experimental data.

References

[1] J. R. Dwyer, M. A. Uman, and H. K. Rassoul, "Remote measurements of thundercloud electrostatic fields," *J. Geophys. Res.*, vol. 114, 2009, Paper D09208. DOI: 10.1029/2008JD011386.

[2] K. B. Eack, "Electrical characteristics of narrow bipolar events," *Geophys. Res. Lett.*, vol. 31, 2004, Paper L20102. DOI: 10.1029/2004GL021117.

[3] A. V. Gurevich, Y. V. Medvedev, and K. P. Zybin, "New type discharge generated in thunderclouds by joint action of runaway breakdown and extensive atmospheric shower," *Phys. Lett. A*, vol. 329, pp. 348–361, 2004.

[4] A. V. Gurevich and K. P. Zybin, "High energy cosmic ray particles and the most powerful discharges in thunderstorm atmosphere," *Phys. Lett. A*, vol. 329, pp. 341–347, 2004.

[5] T. Hamlin, T. E. Light, X. M. Shao, K. B. Eack, and J. D. Harlin, "Estimating lightning channel characteristics of positive narrow bipolar events using intrachannel current reflection signatures," *J. Geophys. Res.*, vol. 112, 2007, Paper D14108. DOI: 10.1029/2007JD008471.

[6] T. Hamlin, K. C. Wiens, A. R. Jacobson, T. E. L. Light, and K. B. Eack, "Space- and ground-based studies of lightning signatures," in *Lightning: Principles, Instruments and Applications,* H. D. Betz, U. Schumann, and P. Laroche, Eds. New York: Springer-Verlag, 2009, pp. 287–307.

[7] D. M. Le Vine, "Sources of the strongest RF radiation from lightning," *J. Geophys. Res.*, vol. 85, pp. 4091–4095, 1980.

[8] A. Nag, V. A. Rakov, and D. Tsalikis, "New experimental data on lightning events producing intense VHF radiation bursts," Eos Trans. AGU, vol. 89, no. 53, Fall Meet. Suppl., Abstract AE11A-0292.

[9] V. A. Rakov, "Initiation of lightning in thunderclouds," *Proc. SPIE*, vol. 5975, pp. 362–373, 2006.

[10] D. A. Smith, M. J. Heavener, A. R. Jacobson, X. M. Shao, R. S. Massey, R. J. Sheldon, and K. C. Weins, "A method for determining intracloud lightning and ionospheric heights from VLF/LF electric field records," *Radio Sci.*, vol. 39, 2004. Paper RS1010. DOI: 10.1029/2002RS002790.

[11] D. A. Smith, X. M. Shao, D. N. Holden, C. T. Rhodes, M. Brook, P. R. Krehbiel, M. Stanley, W. Rison, and R. J. Thomas, "A distinct class of

isolated intracloud discharges and their associated radio emissions," *J. Geophys. Res.*, vol. 104, pp. 4189–4212, 1999.

[12] H. E. Tierney, R. A. Roussel-Dupré, E. M. D. Symbalisty, and W. H. Beasley, "Radio frequency emissions from a runaway electron avalanche model compared with intense, transient signals from thunderstorms," *J. Geophys. Res.*, vol. 110, 2005, Paper D12109. DOI: 10.1029/2004JD005381.

[13] M. A. Uman, *The Lightning Discharge*. New York: Academic, 1987.

[14] S. S. Watson and T. C. Marshall, "Current propagation model for a narrow bipolar pulse," *Geophys. Res. Lett.*, vol. 34, 2007, Paper L04816. DOI: 10.1029/2006GL027426.

[15] J. C. Willett, J. C. Bailey, and E. P. Krider, "A class of unusual lightning electric field waveforms with very strong high-frequency radiation," *J. Geophys. Res.*, vol. 94, pp. 16,255–16,267, 1989.

Amitabh Nag (M'04) received the M.S. degree in electrical engineering in 2007 from the University of Florida, Gainesville, where he is currently working toward the Ph.D. degree.

Since 2005, he has been a Research Assistant at the International Center for Lightning Research and Testing, University of Florida, where he is in charge of the Lightning Observatory. He has authored or coauthored more than 20 papers and technical reports on various aspects of lightning, with 5 papers being published in reviewed journals. His current research interests include measurement, analysis, and modeling of electric and magnetic fields from cloud and ground lightning discharges and lightning detection.

Mr. Nag is a member of the American Meteorological Society and the American Geophysical Union.

Vladimir A. Rakov (SM'96–F'03) received the M.S. and Ph.D. degrees in electrical engineering from Tomsk Polytechnical University (Tomsk Polytechnic), Tomsk, Russia, in 1977 and 1983, respectively.

From 1977 to 1979, he was an Assistant Professor of electrical engineering at Tomsk Polytechnic. In 1978, he also joined the High Voltage Research Institute (a division of Tomsk Polytechnic), where from 1984 to 1994, he was the Director of the Lightning Research Laboratory. He is currently a Professor in the Department of Electrical and Computer Engineering, University of Florida, Gainesville, where he is also the Co-Director of the International Center for Lightning Research and Testing and the Chair of the Electromagnetics and Energy Systems Division. He has authored or coauthored more than 500 publications on various aspects of lightning, with over 160 papers being published in reviewed journals, and has coauthored one book, *Lightning: Physics and Effects*. He is the Editor or an Associate Editor of four technical journals.

Prof. Rakov is the Chairman of the Technical Committee on Lightning of the Biennial International Zurich Symposium on Electromagnetic Compatibility, the Co-Chairman of the International Union of Radio Science (URSI) Working Group (WG) E.4 "Lightning Discharges and Related Phenomena," and the Convener of the International Council on Large Electric Systems (CIGRE) WG C4-407 "Lightning Parameters for Engineering Applications." He is a Fellow of the American Meteorological Society and the Institution of Engineering and Technology.